regions, as predicted from the thermochemical data reported in the literature, are inaccurate.

The solubility of $Cr(OH)_3(s)$ (Figures 2 and 3) indicates that $CrOH^{2+}$ is the dominant Cr species between pH 3.8 and 6.4. Heating the $Cr(OH)_3(s)$ suspensions to 90 °C shows that the Cr concentrations in the suspensions are approximately 2.5 orders of magnitude lower than the Cr concentrations in unheated $Cr(OH)_3(s)$ (Figure 4), indicating the formation of a more ordered solid phase with lower solubility. X-ray diffraction patterns show that the heated solids are amorphous, as were the unheated solids. Heating the $Cr(OH)_3(s)$ suspensions to near boiling is reported to produce crystalline $HCrO_2$ and $Cr_2O_3 \cdot H_2O$.[10,11] Even if $HCrO_2$ and/or $Cr_2O_3 \cdot H_2O$ forms in the suspensions, the aqueous Cr concentrations in equilibrium with the solids would show the same pH dependence as in the case of $Cr(OH)_3(s)$ (eq 1-8). A best-fit straight line through 12 data points between pH 2.6 and 6.0 in Figure 4 has slope -2.00 ± 0.15, indicating (1) that the solubility reaction is similar to that of eq 2 and (2) that Cr^{3+} has no region of dominance above pH 2.6. These findings suggest that the value of the first hydrolysis constant (β_1^*) reported in the literature may be in error and that $CrOH^{2+}$ or some other Cr(III) species that has the same pH dependence as $CrOH^{2+}$ is dominant in the low-pH region.

Although it is not possible to determine the absolute values of equilibrium constants for eq 1, 6, 7, and 8 from these experiments, our results can be used to set upper limits for the constants. Assuming that $Cr_2(OH)_2^{4+}$, $Cr_3(OH)_4^{5+}$, or $Cr_4(OH)_6^{6+}$ becomes dominant at pH 3.8 (the approximate limit of our $Cr(OH)_3(s)$ solubility measurements), the calculated values of log K_{s22}, log K_{s34}, and log K_{s46} in 0.01 M perchlorate are <14.4, <18.5, and <22.4, respectively.

The values of equilibrium constants determined in this study (at 0.01 M ionic strength, and at zero ionic strength as calculated from the Davies[19] equation) are tabulated in Table III, along with the values proposed by Baes and Mesmer,[2] based on a literature review, and Stünzi and Marty.[18] The data given in Table III show that the values obtained in this study for $Cr(OH)_3(s)$ solubility reactions involving different hydrolysis species, especially polynuclear species, are several orders of magnitude less than the values reported in the literature. Because the observed $Cr(OH)_3$ solubility qualitatively confirms the well-known low solubility of $Cr(OH)_3$,[12] the large discrepancy between the observed and the predicted solubility (Figure 3) must be the result of inaccuracies in the values of polynuclear species and/or inaccuracies in extrapolating the values of polynuclear species to low ionic strengths and temperatures.

Acknowledgment. This research was funded by the Electric Power Research Institute, Inc. (EPRI), under contract RP2485-03, titled "Chemical Attenuation Studies". We thank Dr. I. P. Murarka, EPRI project manager, for his support, interest, and helpful suggestions.

(19) Davies, C. W. *Ion Association*; Butterworths: London, 1962.

Contribution from the Instituto de Química, UNAM, Circuito Exterior, Cd. Universitaria, Coyoacan 04510, México, DF, México, and Departamento de Química, Universidad Autonoma Metropolitana, Unidad Iztapalapa, Iztapalapa 09340, México, DF, México

Synthesis, Crystal Structure, and EHMO Calculations for the Nickel(II) Complexes of Imines Derived from Salicylaldehyde, 2-Hydroxy-1-naphthaldehyde, and 3-Hydroxy-2-naphthaldehyde

Juan M. Fernández-G.,*† María J. Rosales-Hoz,† Manuel F. Rubio-Arroyo,† R. Salcedo,† R. A. Toscano,† and A. Vela‡

Received June 16, 1986

The Ni(II) complexes of the imine ligands derived from 2-(aminomethyl)-1,3-dioxolane with salicylaldehyde (**1**), 2-hydroxy-1-naphthaldehyde (**2**), and 3-hydroxy-2-naphthaldehyde (**3**) were synthesized and characterized by elemental analysis, magnetic moments, and infrared and absorption spectra. The structures of the three complexes were determined by single-crystal X-ray diffraction. Crystallographic details for the $C_{22}H_{24}N_2O_6Ni$; are as follows. For **1**: formula $C_{22}H_{24}N_2O_6Ni$; $M_r = 470.7$; space group $P\bar{1}$, with $a = 10.215$ (2) Å, $b = 10.305$ (3) Å, $c = 11.019$ (2) Å, $\alpha = 86.97$ (2)°, $\beta = 69.19$ (2)°, $\gamma = 74.74$ (2)°, and $Z = 2$; $d_{calcd} = 1.497$ g cm^{-3}; μ(Mo Kα) = 9.71 cm^{-1}; $R = 0.044$ for 2119 reflections. For **2**: formula $C_{30}H_{28}N_2O_6Ni$; $M_r = 570.7$; space group $P2_1/c$, with $a = 4.563$ (1) Å, $b = 11.159$ (3) Å, $c = 24.834$ (5) Å, $\beta = 93.21$ (13)°, and $Z = 2$; $d_{calcd} = 1.496$ g cm^{-3}; μ(Mo Kα) = 7.86 cm^{-1}; $R = 0.042$ for 1684 reflections. For **3**: formula $C_{30}H_{28}N_2O_6Ni$; $M_r = 570.7$; space group $P2_1/n$, with $a = 13.677$ (5) Å, $b = 5.585$ (2) Å, $c = 17.267$ (5) Å, $\beta = 93.06$ (3)°, and $Z = 2$; $d_{calcd} = 1.439$ g cm^{-3}; μ(Mo Kα) = 7.84 cm^{-1}; $R = 0.048$ for 1388 reflections. The metal is placed in a center of symmetry in all three cases with square-planar coordination. Compounds **1** and **3** deviate from planarity in a stepped fashion. The height of the step and the magnitude of some interatomic distances in the chelate rings, particularly Ni-N, are analyzed in terms of steric and electronic effects. EHMO calculations were carried out in order to evaluate some of these effects.

Introduction

Metal derivatives of Schiff-base ligands have been extensively studied for a long time[1] and the chemistry of bis(bidentate Schiff-base)copper(II) and -nickel(II) complexes has been particularly enriched by many contributions in both synthetic and structural areas.[2-4] These studies have shown that while in the solid state the structure of these complexes may lie anywhere between square planar and tetrahedral with other intermediate structures also being found (mainly stepped and umbrella-shaped square-planar conformations), in solution several of these conformations can exist in equilibrium.[4,5] This variety of structures has been interpreted in terms of both steric[4] and electronic[6] factors.

The differences in structure (planar or tetrahedral) of copper and nickel bis(substituted salicylaldimines) have been observed to affect the expression for the rate of ligand substitution process.[7] Furthermore, a relationship can be drawn between the steric bulk of the N substituents and the relative importance of the solvent-

†UNAM.
‡Universidad Autonoma Metropolitana.

(1) Sacconi, L. *Coord. Chem. Rev.* **1966**, *1*, 126.
(2) Holm, R. H.; Everett, G. W. Jr.; Chakravorty, A. *Prog. Inorg. Chem.* **1966**, *7*, 83.
(3) Yamada, S.; Takeuchi, A. *Coord. Chem. Rev.* **1982**, *43*, 187.
(4) Holm, R. H.; O'Connor, M. J. *Prog. Inorg. Chem.* **1971**, *14*, 841.
(5) Cariati, F.; Ganadu, M. L.; Zoroddu, A.; Mansani, R.; Quidacciolu, R. *Inorg. Chem.* **1985**, *24*, 4030.
(6) Maslen, H. S.; Waters, T. N. *Coord. Chem. Rev.* **1975**, *17*, 137.
(7) Schumann, M.; Elias, H. *Inorg. Chem.* **1985**, *24*, 3187.

0020-1669/87/1326-0349$01.50/0

and ligand-dependent contributions in the substitution rate law.[8]

An estimation of the influence of the electronic factor in those systems could be achieved through comparative studies of analogous complexes derived from salicylaldimines and the corresponding 2-hydroxy-1-naphthaldimines and 3-hydroxy-2-naphthaldimines where there are intrinsic aromaticity differences that could be reflected in some structural features of the complexes.

There are, however, few structural data for metal derivatives of 2-hydroxy-1-naphthaldimines[9,10] and, to our knowledge, only one structural report for a 3-hydroxy-2-naphthaldimine complex.[11]

We have previously[11] described the crystal and molecular structure of three Ni(II) Schiff-base complexes derived from salicylaldehyde (sal), 2-hydroxy-1-naphthaldehyde (1,2-naph), and 3-hydroxy-2-naphthaldehyde (2,3-naph). In these compounds, the variation in the Ni–N bond lengths seems to follow the same trend observed by Calvin and Wilson[12] for the stability constants of copper(II)–phenolate and –naphtholate complexes (Cu–1,2-naph > Cu–sal > Cu–2,3-naph). However some amount of disorder in the N substituent lowered the precision of the results.

In order to observe if this trend is really followed and to try to quantify the degree of electron delocalization in the compounds, we prepared and characterized by spectroscopic techniques and X-ray analysis the complexes bis[*N*-((1,3-dioxolan-2-yl)-methyl)salicylaldiminato]nickel(II) (**1**), bis[*N*-((1,3-dioxolan-2-yl)methyl)-2-hydroxy-1-naphthaldiminato]nickel(II) (**2**), and bis[*N*-((1,3-dioxolan-2-yl)methyl)-3-hydroxy-2-naphthaldiminato]nickel(II), (**3**) and carried out extended Hückel molecular orbital calculations on them. The results are reported herein.

Experimental Section

General Information. Melting points were determined in a Fisher-Jones melting point apparatus and are uncorrected; infrared spectra were recorded on a Perkin-Elmer Model 283-B spectrometer and UV–visible spectra on a Perkin-Elmer Model 552 spectrophotometer; mass spectra were obtained by using a Hewlett-Packard instrument, Model 5985, at 70-eV ionizing potential; magnetic moment measurements were made with a Cahn electromagnet, Model 6685, and a Cahn 2000 electrobalance at 23 °C. Elemental analyses were performed by Dr. E. Pascher in Bonn, Federal Republic of Germany.

Synthesis. Nickel acetate tetrahydrate, diglyme, salicylaldehyde, and 2-hydroxy-1-naphthaldehyde were from Aldrich and were used without further purification; 3-hydroxy-2-naphthaldehyde was prepared as described in the literature[13] with Naphthol AS (Koch & Light Labs Ltd) used as the starting material; 2-(aminomethyl)-1,3-dioxolane was obtained from 2-(bromomethyl)-1,3-dioxolane (Aldrich) and ammonia under pressure.[14]

The nickel complexes were prepared by methods described elsewhere,[15] by the reaction between the monoanion of the preformed ligand and nickel acetate. The following preparation is a typical example of the general method. To a solution of 344 mg (2 mmol) of 2-hydroxy-1-naphthaldehyde in 100 mL of absolute methanol was added 236 mg (2 mmol) of 2-(aminomethyl)-1,3-dioxolane was added. The solution was refluxed for 30 min and then cooled to room temperature. A solution of 118 mg of potassium hydroxide in 60 mL of methanol was then added, followed by addition of 273 mg (1.1 mmol) of nickel acetate tetrahydrate in 75 mL of methanol. The reaction mixture was refluxed for 30 min and concentrated until a precipitate was observed; the green solid was filtered with suction, washed with cold water, and dried. Recrystallization from dichloromethane–methanol gave 300 mg of deep green crystals of complex **2**, mp 257–259 °C.

Table I. Summary of Crystal Data, Intensity Data Collection, and Structure Refinement

	1	**2**	**3**
molecular formula	$C_{22}H_{24}N_2O_6Ni$	$C_{30}H_{28}N_2O_6Ni$	$C_{30}H_{28}N_2O_6Ni$
M_R	470.7	570.7	570.7
cryst dimens, mm	0.28 × 0.3 × 0.4	0.46 × 0.29 × 0.17	0.24 × 0.36 × 0.3
cryst syst	triclinic	monoclinic	monoclinic
space group	$P\bar{1}$	$P2_1/c$	$P2_1/n$
cell dimens			
a, Å	10.215 (2)	4.563 (1)	13.677 (5)
b, Å	10.305 (3)	11.159 (3)	5.585 (2)
c, Å	11.019 (2)	24.834 (5)	17.267 (5)
α, deg	86.97 (2)	90	90
β, deg	69.19 (2)	93.21	93.06
γ, deg	74.74 (2)	90	90
V, Å^3	1044.9 (4)	1262.19	1317.1 (1)
D_c, g cm^{-3}	1.497	1.501	1.439
Z	2	2	2
$F(000)$	492	596	596
λ, Å	0.71069	0.71069	0.71069
μ(Mo Kα), cm^{-1}	9.71	7.86	7.84
diffractometer	Nicolet	Stoe	Nicolet
$2\theta_{min}$, deg	3	5	3
$2\theta_{max}$, deg	45	50	45
no. of reflcns measd	2720	3999	1706
no. of unique reflcns	2199	1684	1388
G limit $\|F > n\sigma(F)\|$, n	3	4	3
weighting sch	$[\alpha^2(F_o) + 0.006F^2]^{-1}$	$[\alpha^2(F_o) + 0.002F^2]^{-1}$	$[\alpha^2(F_o) + 0.002F^2]^{-1}$
converged residuals			
R	0.0435	0.0423	0.0481
R_w	0.0419	0.0426	0.0537

Table II. Extended Hückel Parameters

orbital	H_{ii}, eV	exponents[a] ξ_1	ξ_2
H_{1s}	−13.60	1.3	
C_{2s}	−21.40	1.625	
C_{2p}	−11.40	1.625	
N_{2s}	−26.00	1.950	
N_{2p}	−13.40	1.950	
O_{2s}	−32.30	2.275	
O_{2p}	−14.80	2.275	
Ni_{4s}	−8.86	1.825	
Ni_{4p}	−4.90	1.125	
Ni_{3d}	−11.50	5.75 (0.5683)	2.0 (0.6292)

[a] Two Slater exponents are listed for 3d functions. Each is followed in parentheses by the coefficient in the double-ζ expansion.

Structure Determination. Crystallographic Data Collection and Refinement of the Structures. Crystals of the compounds **1** and **2** were grown by slow evaporation of CH_2Cl_2–THF–CH_3OH; those of **3** were grown from diglyme–benzonitrile. The unit cells for compounds **1** and **3** were obtained from 25 and 15 reflections ($3° < 2\theta < 20°$), respectively. The data were collected on a Nicolet R3m four-circle diffractometer with graphite-monochromated Mo Kα radiation, using an ω scan mode with variable scan rate from 4 to 30 deg/min and a scan width of 1.0°. Agreement factors for equivalent reflections for **1–3** were 0.0196, 0.0209, and 0.0208 respectively. Maximum and minimum transmission factors for absorption corrections for **2** were 0.8905 and 0.7939, respectively.

The space group and approximate cell dimensions for **2** were determined via Weissenberg (Cu Kα) X-ray photography. The crystal was then transferred to a Stoe diffractometer, and accurate cell dimensions were determined from the angular measurement of 15 strong reflections in the range $15 < 2\theta < 25°$. Data collection for compound **2** was carried out at room temperature by using an ω/θ scan mode. Although the crystal was known to belong to a monoclinic space group, a full hemisphere of data was collected ($+h,\pm k,\pm l$) to improve the statistical quality of data. For the data collection of **2**, the step width was set at 0.05° and the time for each step varied from 0.75 to 4.00 s, depending on the intensity recorded in a prescan. The intensity data were profile fitted "on line" by using the method of Clegg.[16] A numerical absorption correction

(8) Elias, H.; Hasserodt-Taliaferro, C.; Hellriegel, L.; Schonherr, W.; Wannowis, K. J. *Inorg. Chem.* **1985**, *24*, 3192.
(9) Von Freiburg, C.; Reichert, W.; Melchers, M.; Engelen, B. *Acta Crystallogr., Sect. B: Struct. Crystallogr. Cryst. Chem.* **1980**, *B36*, 1209.
(10) (a) Martin, D. W.; Waters, T. N. *J. Chem. Soc., Dalton Trans.* **1973**, 2440. (b) Clark, G. R.; Waters, J. M.; Waters, T. N. *J. Inorg. Nucl. Chem.* **1975**, *37*, 2455. (c) Clark, G. R.; Waters, J. M.; Waters, T. N.; Williams, G. J. *J. Inorg. Nucl. Chem.* **1977**, *39*, 1971.
(11) Fernández-G., J. M.; Rosales-Hoz, M.; Toscano, R. A.; Tapia-T., R. G. *Acta Crystallogr., Sect. C: Cryst. Struct. Commun.* **1986**, *C42*, 1313.
(12) Calvin, M.; Wilson, K. W. *J. Am. Chem. Soc.* **1945**, *67*, 2003.
(13) Khorana, M. L.; Pandit, S. Y. *J. Indian Chem. Soc.* **1963**, *40*, 789.
(14) Woodward, R. B.; Doering, W. E. *Organic Syntheses*; Wiley: New York, 1966; Collect. Vol. III, p 50.
(15) Yamada, S.; Kuge, K.; Yamagouchi, K. *Bull. Chem. Soc. Jpn.* **1967**, *40*, 1864.
(16) Clegg, W. *Acta Crystallogr., Sect. A: Cryst. Phys., Diffr., Theor. Gen. Crystallogr.* **1981**, *A37*, 22.

Table III. Analytical Data and Other Properties of **1–3**

compd	color	mp, °C	magn propts[a]	M^+, m/e	$\nu_{C=N}$, cm^{-1}	anal.,[b] % C	H	N	vis–UV abs bands[c] ν_{max}, cm^{-1} (ϵ, M^{-1} cm^{-1})
1	green	225–227	diamag	470	1612	55.82 (56.08)	4.95 (5.09)	5.72 (5.94)	16 420 (73), 24 271 (4583), 30 675 (9084), 3713 (43354), 40 983 (48 515)
2	green	257–259	diamag	570	1617	62.39 (63.08)	5.03 (4.91)	5.11 (4.91)	16 835 (128), 23 696 (3208), 30 211 (8480), 32 680 sh, 36 630 (43 544)
3	brown	>300	diamag	dec	1615	62.86 (63.08)	4.74 (4.91)	4.65 (4.91)	16 556 (61), 20 333 sh, 22 831, 28 490, 34 483, 39 370

[a] At 23 °C. [b] Calculated values in parentheses. [c] Anhydrous diglyme was used as solvent.

Table IV. Atom Coordinates ($\times 10^3$) for Complexes **1–3**

	x				*y*				*z*			
	1a	**1b**	**2**	**3**	**1a**	**1b**	**2**	**3**	**1a**	**1b**	**2**	**3**
Ni	0	5000	10000	0	0	0	5000	0	5000	5000	5000	10000
N(1)	718 (4)	5778 (4)	12447 (6)	928 (2)	1486 (4)	1537 (3)	5705 (2)	−2615 (6)	4191 (3)	4750 (3)	4486 (1)	9942 (2)
O(1)	−1309 (3)	3153 (3)	8881 (6)	275 (2)	1044 (3)	1023 (3)	3786 (2)	1101 (6)	6427 (3)	5835 (3)	4536 (1)	9039 (2)
O(2)	1419 (4)	6515 (4)	11034 (7)	2223 (2)	2552 (4)	2626 (3)	8036 (2)	−3333 (7)	1420 (3)	2093 (3)	4005 (1)	11848 (2)
O(3)	3217 (4)	8607 (4)	13533 (6)	2802 (2)	613 (3)	1027 (4)	8944 (2)	−1657 (7)	836 (3)	1523 (3)	4699 (1)	10771 (2)
C(1)	−1309 (4)	3632 (4)	11564 (8)	1444 (3)	3228 (4)	3070 (4)	4247 (3)	−3553 (8)	5576 (4)	6261 (4)	3763 (1)	7918 (3)
C(2)	−1896 (4)	2710 (4)	9646 (8)	1076 (3)	2360 (4)	2234 (4)	3546 (3)	−2385 (7)	6510 (4)	6402 (4)	4049 (1)	8546 (2)
C(3)	−3135 (5)	1231 (5)	8397 (9)	590 (3)	2898 (4)	2725 (4)	2482 (3)	−138 (8)	7596 (4)	7155 (4)	3807 (2)	8442 (3)
C(4)	−3782 (5)	703 (5)	9070 (9)	473 (3)	4255 (5)	3996 (5)	2154 (3)	779 (8)	7722 (4)	7736 (4)	3302 (2)	7695 (3)
C(5)	−3231 (5)	1621 (5)	11699 (10)	724 (3)	5136 (5)	4823 (5)	2478 (4)	518 (8)	6791 (4)	7616 (4)	2471 (2)	6288 (3)
C(6)	−2005 (5)	3053 (5)	13554 (11)	1105 (3)	4622 (4)	4370 (4)	3127 (4)	−653 (10)	5732 (4)	6883 (4)	2181 (2)	5678 (3)
C(7)	21 (4)	5103 (4)	14793 (11)	1597 (3)	2739 (4)	2692 (4)	4180 (4)	−2849 (10)	4511 (4)	5304 (4)	2400 (2)	5792 (3)
C(8)	2109 (4)	7234 (4)	14152 (9)	1708 (3)	1269 (4)	1460 (4)	4568 (4)	−3820 (10)	3091 (4)	3770 (4)	2905 (2)	6516 (3)
C(9)	1883 (5)	7209 (4)	12250 (8)	1327 (3)	1244 (4)	1374 (4)	3904 (3)	−2642 (8)	1819 (4)	2426 (4)	3220 (1)	7167 (3)
C(10)	2526 (7)	7127 (7)	11009 (9)	834 (3)	2776 (6)	2616 (6)	2844 (3)	−401 (8)	323 (5)	723 (5)	2998 (1)	7047 (3)
C(11)	3357 (7)	8573 (7)	12857 (7)	1260 (3)	1428 (6)	1676 (6)	5296 (3)	−3396 (8)	−239 (5)	365 (5)	4007 (1)	9311 (3)
C(12)			14036 (7)	1303 (3)			6834 (3)	−3833 (9)			4613 (1)	10657 (3)
C(13)			12003 (8)	1936 (3)			7897 (2)	−2192 (9)			4547 (1)	11147 (2)
C(14)			10581 (13)	3245 (4)			9286 (3)	−3019 (11)			3934 (2)	11984 (3)
C(15)			12261 (12)	3520 (3)			9875 (3)	−1308 (11)			4371 (2)	11376 (3)

is of the Gaussian type based on the planes |100|, |011|, |011|, |010|, and |001|.[18] Crystal data and additional data collection parameters are given in Table I.

The structure of **2** was solved by the conventional heavy-atom method and subsequent electron density difference syntheses while those of **1** and **3** were solved by direct methods and Fourier difference maps. The three structures were refined by the full-matrix least-squares method using anisotropic thermal parameters for all non-hydrogen atoms. Hydrogen atoms were placed in idealized positions and included in the refinement.

The atomic scattering factors were taken from the ref 17. In the case of compound **2**, the preliminary data reduction was performed on a Nova 3 computer using programs written by Dr. W. Clegg[16] and structure solution and refinement was performed on the University of Cambridge IBM 3081 computer using the SHELX-76 package.[18] The solution and refinement of structures **1** and **3** was carried out by using SHELXTL[19] on a Nova 4S computer.

Theoretical Calculations. All calculations were carried out with the extended Hückel method.[20] A weighted H_{ij} formula was used in all calculations.[21] Valence state ionization potentials H_{ii} are shown in Table II. The value for nickel 3d orbital was calculated by the method described in the Appendix; Basch and Gray orbitals were used for the Nickel functions.[22] The parameters for C, N, O, and H are standard ones. The ICON-8 program (extended Hückel) was adapted for working with more than 50 atoms and to compile in the 7800 Burroughs computer used.

Results

Some physical properties of the synthesized compounds are listed in Table III. Surprisingly, complex **3** was very insoluble while compounds **1** and **2** were soluble in dichloromethane or chloroform and slightly soluble in the other usual organic solvents. The elemental analyses show the complexes to have a 2:1 lig-

Table V. Bond Lengths (Å) for Complexes **1–3**

	1a	**1b**	**2**	**3**
Ni–N(1)	1.913 (4)	1.918 (4)	1.912 (3)	1.941 (3)
Ni–O(1)	1.829 (2)	1.828 (2)	1.832 (2)	1.828 (3)
O(1)–C(2)	1.323 (5)	1.318 (5)	1.305 (4)	
O(1)–C(3)				1.332 (5)
O(2)–C(9)	1.409 (6)	1.398 (5)		
O(2)–C(10)	1.389 (7)	1.412 (6)		
O(2)–C(13)			1.401 (4)	1.406 (5)
O(2)–C(14)			1.419 (4)	1.416 (6)
O(3)–C(9)	1.419 (5)	1.384 (5)		
O(3)–C(11)	1.402 (7)	1.416 (6)		
O(3)–C(13)			1.402 (3)	1.383 (6)
O(3)–C(15)			1.424 (4)	1.408 (6)
N(1)–C(7)	1.298 (5)	1.302 (5)		
N(1)–C(8)	1.475 (5)	1.480 (5)		
N(1)–C(11)			1.297 (4)	1.279 (6)
N(1)–C(12)			1.479 (3)	1.478 (6)
C(1)–C(2)	1.402 (6)	1.401 (7)	1.397 (5)	1.383 (6)
C(1)–C(6)	1.414 (5)	1.416 (6)		
C(1)–C(7)	1.430 (5)	1.429 (4)		
C(1)–C(9)			1.453 (5)	1.393 (6)
C(1)–C(11)			1.429 (4)	
C(2)–C(3)	1.402 (5)	1.406 (5)	1.434 (4)	1.427 (6)
C(2)–C(11)				1.446 (6)
C(3)–C(4)	1.371 (6)	1.374 (6)	1.358 (5)	1.388 (6)
C(4)–C(5)	1.398 (7)	1.395 (8)		
C(4)–C(10)			1.421 (5)	1.410 (6)
C(5)–C(6)	1.374 (5)	1.361 (6)	1.352 (6)	1.365 (7)
C(5)–C(10)			1.423 (5)	1.410 (6)
C(6)–C(7)			1.401 (6)	1.408 (8)
C(7)–C(8)			1.373 (5)	1.364 (7)
C(8)–C(9)	1.502 (7)	1.498 (6)	1.412 (5)	1.425 (7)
C(9)–C(10)			1.410 (5)	1.431 (6)
C(10)–C(11)	1.459 (8)	1.466 (8)		
C(12)–C(13)			1.509 (4)	1.492 (6)
C(14)–C(15)			1.450 (6)	1.483 (8)

(17) *International Tables for X-Ray Crystallography*; Kynoch: Birmingham, England, 1974; Vol. IV, pp 72–98.
(18) Sheldrick, G. M. "SHELX 76, Crystal Structure Solving Package", University of Cambridge, 1976.
(19) Sheldrick, G. M. "SHELXTL Version 3, An Integrated System for Solving, Refining and Displaying Crystal Structures from Diffraction Data", University of Gottingen, Federal Republic of Germany, 1981.
(20) (a) Hoffmann, R. *J. Chem. Phys.* **1963**, *39*, 1397. (b) Hoffmann, R.; Lipscomb, W. N. *Ibid.* **1962**, *36*, 3179, 3489. (c) *Ibid.* **1962**, *37*, 2872.
(21) Ammeter, J. H.; Burgi, H. B.; Thibeault, J. C.; Hoffmann, R. *J. Am. Chem. Soc.* **1978**, *100*, 3686.
(22) Basch, H.; Gray, H. B. *Theor. Chim. Acta* **1966**, *4*, 367.

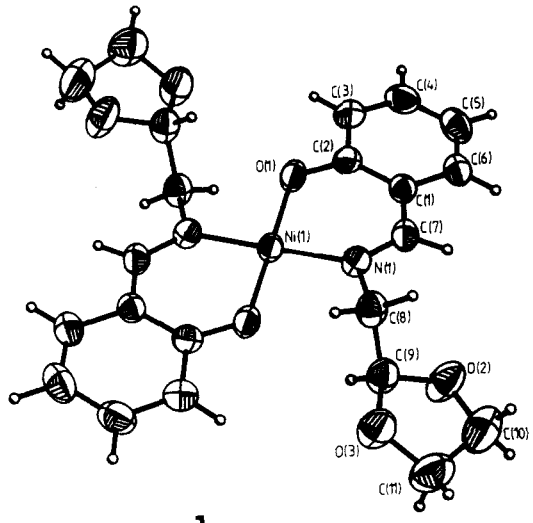

1a

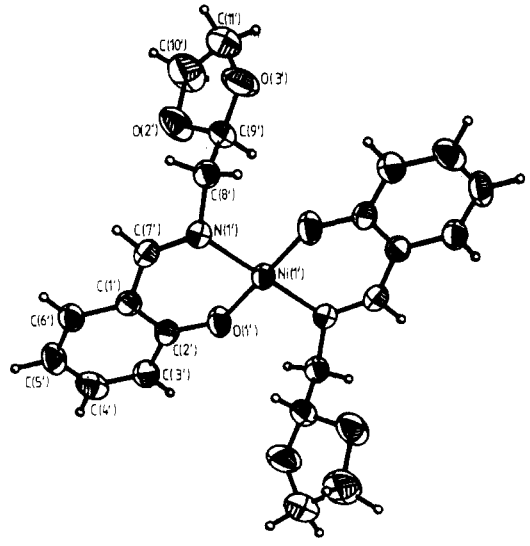

1b

Figure 1. ORTEP diagrams of the two molecules of compound **1** drawn at 50% probability.

and-to-metal ratio. For the three complexes the frequency for the $\nu_{C=N}$ vibration band is found in the usual range around 1600–1650 cm^{-1}.[23] Diamagnetism of the complexes indicate that the coordination of the nickel atom is square planar. Except in that for **3**, the mass spectra of the complexes show the expected molecular ion, with the characteristic metal isotopic contribution, which agrees with the 2:1 ligand to metal stoichiometry. They follow the fragmentation patterns reported for structurally related complexes.[24] Compound **3** decomposes before entering the ionization chamber.

The UV–visible spectra of the complexes show bands (Table II) that could be assigned to transitions characteristic of similar Schiff-base–nickel(II) square-planar complexes.[25a]

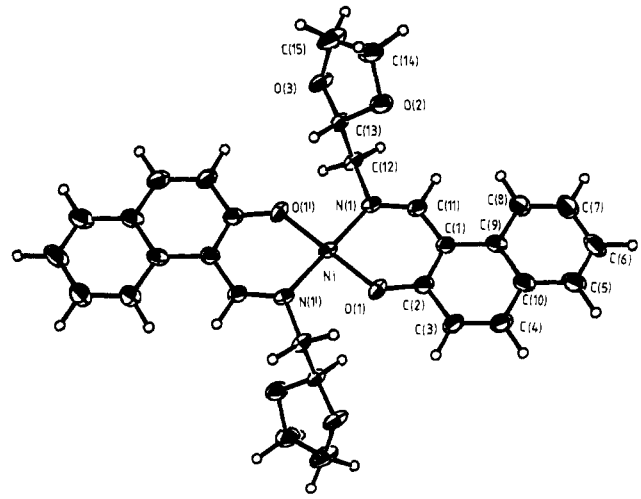

Figure 2. ORTEP diagram of compound **2**.

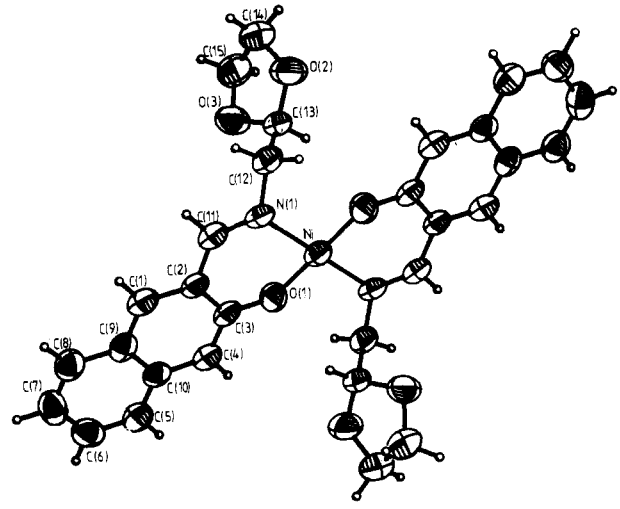

Figure 3. ORTEP diagram of compound **3**.

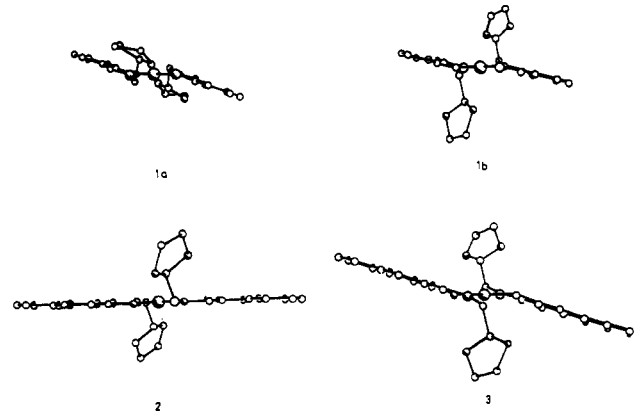

Figure 4. Side view of the four molecules of compounds **1–3**.

Structural Results. Final positional parameters for compounds **1–3** are given in Table IV. Tables V and VI contain bond lengths and angles. In the three compounds each ligand molecule binds bidentately and the nickel atoms lie on centers of symmetry, thereby imposing a square-planar coordination around the metal atoms (Figures 1–3).

The asymmetric unit of compound **1** contains two distinct half-molecules of the complex. The two molecules are very similar, the only difference being found in the conformation of the oxygen-containing five-membered ketal ring. In one molecule the ring is almost parallel to the aromatic-chelate plane (**1a**) while in the other one (**1b**) a larger angle with the rest of the ligand is observed.

(23) Teyssie, P.; Charette, J. J. *Spectrochim. Acta* **1963**, *19*, 1407.
(24) Fernández-G., J. M.; Cortes, E.; Gomez-Lara, J. *J. Inorg. Nucl. Chem.* **1975**, *37*, 1385.
(25) (a) Waters, T. N.; Wright, P. E. *J. Inorg. Nucl. Chem.* **1971**, *33*, 359. (b) Kato, H.; Sakamoto, T. *J. Am. Chem. Soc.* **1974**, *96*, 4131. (c) Lever, A. B. P. *Inorganic Electronic Spectroscopy*; Elsevier: New York, 1968; pp 343–345.

Table VI. Bond Angles (deg) of Complexes **1–3**

	1a	**1b**	**2**	**3**
C(3)–C(4)–C(5)	121.6 (4)	121.0 (4)		
C(3)–C(4)–C(10)			121.7 (3)	122.4 (4)
C(4)–C(5)–C(6)	118.7 (4)	119.1 (3)		
C(6)–C(5)–C(10)			121.0 (4)	121.1 (4)
C(5)–C(6)–C(7)			119.5 (4)	120.6 (5)
C(1)–C(6)–C(5)	121.1 (4)	121.4 (5)		
C(6)–C(7)–C(8)			121.2 (1)	120.2 (5)
C(7)–C(8)–C(9)			120.7 (4)	120.8 (5)
C(1)–C(9)–C(8)			123.2 (3)	122.5 (4)
C(1)–C(9)–C(10)			118.8 (3)	118.9 (4)
C(8)–C(9)–C(10)			118.0 (3)	110.6 (4)
C(4)–C(10)–C(5)			120.7 (3)	122.9 (4)
C(4)–C(10)–C(9)			119.6 (3)	118.4 (4)
C(5)–C(10)–C(9)			119.7 (4)	118.7 (4)
N(1)–C(7)–C(1)	126.3 (4)	126.2 (4)		
N(1)–C(11)–C(1)			126.8 (3)	
N(1)–C(11)–C(2)				126.3 (4)
N(1)–C(8)–C(9)	110.9 (4)	110.4 (4)		
N(1)–C(12)–C(13)			110.8 (3)	110.8 (4)
O(2)–C(9)–O(3)	106.7 (3)	106.6 (3)		
O(2)–C(13)–O(3)			107.0 (2)	106.8 (3)
O(2)–C(9)–C(8)	111.7 (4)	110.5 (3)		
O(2)–C(13)–C(12)			110.6 (3)	109.7 (4)
O(3)–C(9)–C(8)	109.5 (4)	110.5 (4)		
O(3)–C(13)–C(12)			109.4 (3)	110.2 (4)
O(2)–C(10)–C(11)	104.1 (5)	105.8 (5)		
O(2)–C(14)–C(15)			106.6 (3)	104.3 (4)
O(3)–C(11)–C(10)	104.3 (4)	105.1 (4)		
O(3)–C(15)–C(14)			106.2 (3)	104.1 (4)
N(1)–Ni–O(1)	92.5 (1)	92.3 (1)	92.1 (1)	92.3 (1)
O(1)–Ni–N(1a)	87.5 (1)	87.7 (1)	87.9 (1)	87.7 (1)
O(1)–Ni–O(1a)	180.0	180.0	180.0	180.0
Ni–N(1)–C(7)	124.0 (3)	124.4 (3)		
Ni–N(1)–C(8)	121.0 (3)	120.0 (2)		
Ni–N(1)–C(11)			126.0 (2)	124.3 (3)
Ni–N(1)–C(12)			120.3 (2)	120.1 (3)
C(7)–N(1)–C(8)	114.9 (4)	115.6 (4)		
C(11)–N(1)–C(12)			113.7 (3)	115.7 (6)
Ni–O(1)–C(2)	128.3 (3)	129.3 (3)	130.9 (2)	
Ni–O(1)–C(3)				128.2 (3)
C(9)–O(2)–C(10)	108.3 (4)	104.9 (3)		
C(9)–O(3)–C(11)	106.7 (3)	107.5 (4)		
C(13)–O(2)–C(14)			105.3 (3)	108.3 (4)
C(13)–O(3)–C(15)			105.8 (3)	104.9 (3)
C(2)–C(1)–C(6)	119.2 (3)	119.3 (4)		
C(2)–C(1)–C(7)	121.1 (3)	120.8 (4)		
C(2)–C(1)–C(9)			119.9 (3)	121.9 (4)
C(1)–C(2)–C(3)	119.2 (4)	118.4 (4)	119.8 (3)	120.2 (4)
C(2)–C(1)–C(11)			119.9 (3)	
C(3)–C(2)–C(11)				121.0 (4)
C(6)–C(1)–C(7)	119.6 (4)	119.5 (4)		
C(1)–C(2)–C(11)				118.6 (4)
C(9)–C(1)–C(11)			120.2 (3)	
O(1)–C(2)–C(1)	122.7 (3)	123.2 (3)	124.3 (3)	
O(1)–C(3)–C(2)				121.8 (4)
O(1)–C(2)–C(3)	118.1 (4)	118.3 (4)	115.9 (3)	
O(1)–C(3)–C(4)				120.1 (4)
C(2)–C(3)–C(4)	120.2 (4)	120.7 (5)	120.3 (3)	113.1 (4)

Bond lengths and angles in complex **1** are similar to those observed in other (salicylideniminato)nickel compounds.[26,27] Both molecules of **1** have a stepped conformation with a larger step in **1a** than in **1b**. The nickel atom is 0.423 Å out of the aromatic plane in **1a** but only 0.205 Å out of the same plane in **1b**.

Few metal complexes containing 1,2-naphthaldimine ligands have been described, most of them copper compounds.[9,10,28] The Ni–N bond in compound **2** (1.912 [31 Å) is longer than the corresponding value in a *cis*-(naphthaldiminato)nickel complex

Table VII. Orbital Occupation in the Metal

	orbital	
compd	$d_{x^2-y^2}$	d_{yz}
1a	0.709	1.751
1b	0.785	1.705
2	0.570	1.958
3	0.736	1.801

Table VIII. Overlap Population for the Chelate Ring in Compounds **1–3**

bond	overlap	**1a**	**1b**	**2**	**3**
C–N	σ	0.862	0.882	0.752	0.750
	π	0.236	0.222	0.348	0.382
	tot.	1.098	1.104	1.100	1.132
C–O	σ	0.602	0.594	0.641	0.586
	π	0.115	0.116	0.096	0.112
	tot.	0.717	0.710	0.737	0.698
Ni–N	σ	0.288	0.278	0.303	0.299
	π	0.046	0.058	0.030	0.026
	tot.	0.334	0.336	0.333	0.325
Ni–O	σ	0.275	0.274	0.273	0.271
	π	−0.009	−0.009	−0.007	−0.005
	tot.	0.266	0.265	0.266	0.266

that has been previously described (1.836 [3] Å), but this difference is probably an effect of the cis–trans isomerism. The corresponding value in a similar trans compound is not significantly different.[11]

Compound **2** is practically planar with the nickel atom just 0.073 Å out of the naphthalene least-squares plane. This is different from what had been observed in other 1,2-naph complexes where step heights as high as 1.26 Å have been observed.

As far as we know no other metal complexes containing the 2,3-naph moiety have been characterized by X-ray diffraction apart from an ethoxyethylamine derivative prepared by us.[11] Bond lengths and angles are quite similar between that compound and **3**. The molecule of **3** also shows a stepped conformation with the metal atom 0.374 Å out of the plane defined by the aromatic rings. All three complexes show very similar values for the "bite" angle N–M–O [92.4 (1), 92.1 (1), and 92.3 (1)°]. The angle at oxygen is slightly larger in **2** than in **1** or **3** and so is the angle at the carbon atom bonded to the oxygen. All the other angles in the chelate ring are similar in the three compounds.

On the other hand there is a significant difference between the Ni–N bond lengths of compounds **2** and **3** with values of 1.912 (3) Å for **2** and 1.941 (3) Å for **3**. Similar differences have been observed in several copper–salicylaldimines,[29] but in those cases the group bonded to the nitrogen atom varied largely from one compound to the other while in **2** and **3** this group remains constant. In **1** the value for this distance (average 1.915 Å) is practically the same than that in **2**, but in the ethoxyethylamine derivatives already discussed,[11] the Ni–N distance in the salicylaldimine derivative is similar to that in the 2,3-naphthaldimine compound.

There are no differences in the Ni–O bond lengths. Compound **2** shows slightly shorter O–C distances than **1** and **3**, especially with that in **3**.

Bond lengths and angles in the naphthalene rings (with the exception of C(1)–C(9)) are very similar in compounds **2** and **3**, and both show some differences from naphthalene itself as expected for a chelate derivative.[30]

There are some short intramolecular contacts (1.963–1.971 Å) between the ketal oxygen atoms and some carbon-bonded hydrogen atoms in **1a** and **1b**. These interactions may be partly responsible for the different arrangements of the five-membered rings in the two molecules found in the asymmetric unit of the compound **1**.

EHMO Calculation Results. The main object of this section is to determine the electronic structure and the interaction and

(26) Skolnikova, L. M.; Kryazeva, A. N.; Voblikova, V. A. *Acta Crystallogr., Sect. A: Cryst. Phys., Diffr., Theor. Gen. Crystallogr.* **1966**, *21A*, 152.
(27) Bhatia, S. C.; Bindlish, J. M.; Saini, A. R.; Jain, P. C. *J. Chem. Soc., Dalton Trans.* **1981**, 1773.
(28) (a) Matsumoto, N.; Nonaka, Y.; Kida, S.; Kawano, S.; Ueda, J. *Inorg. Chim. Acta* **1979**, *37*, 27. (b) Matsumoto, N.; Miyazaki, T.; Sagara, Y.; Ohyoshi, A. *Inorg. Chim. Acta* **1982**, *63*, 249.
(29) Cruickshank, D. W. J. *Acta Crystallogr.* **1957**, *10*, 504.
(30) Jain, P. C.; Syal, V. K. *J. Chem. Soc., Dalton Trans.* **1973**, 1908.

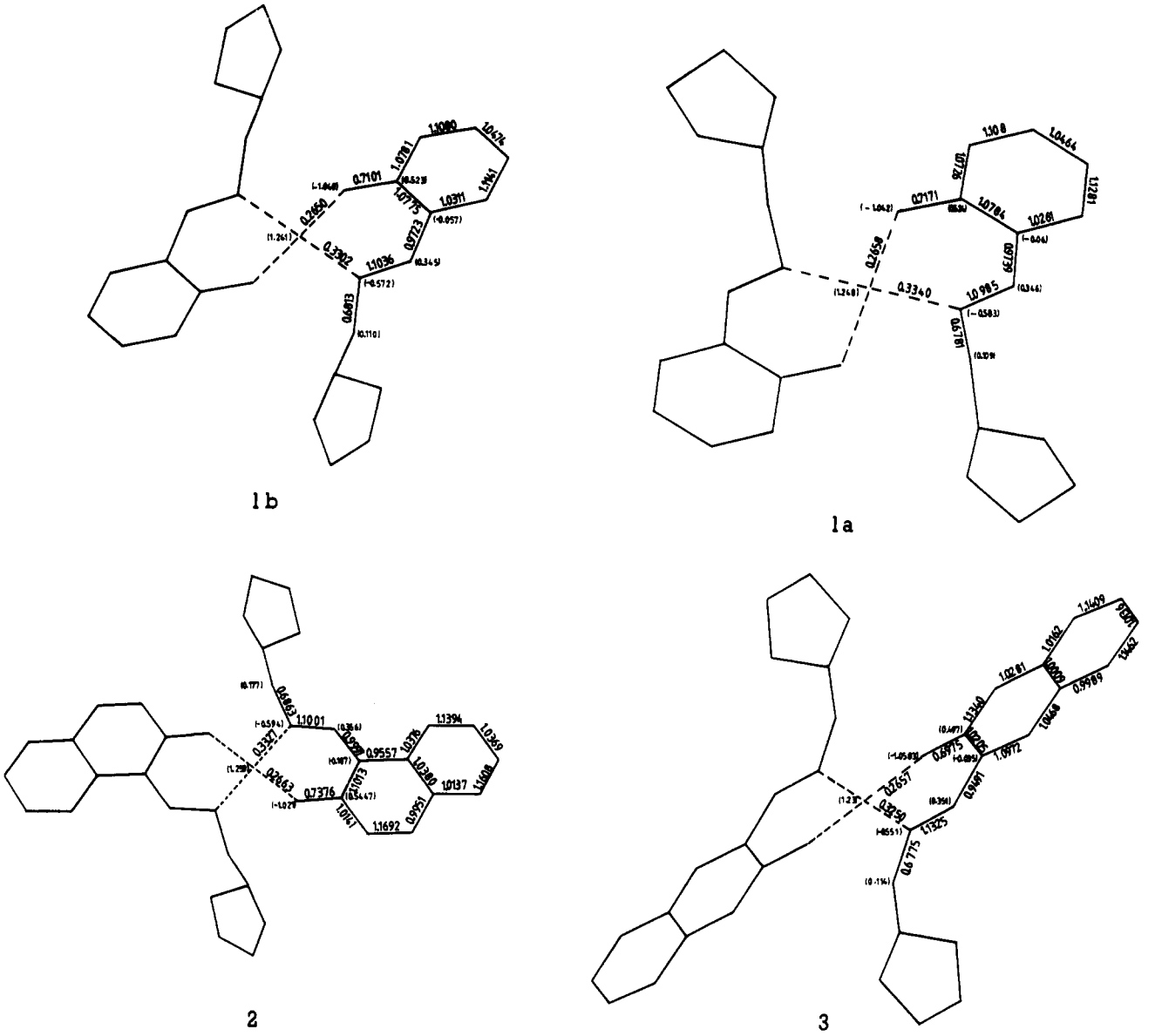

Figure 5. Overlap populations and net atom charges for **1a**, **1b**, **2**, and **3**.

contour diagrams for the orbitals in molecules **1a**, **1b**, **2**, and **3** and to relate these results with other properties shown by the complexes. Molecular orbital calculations at the extended Hückel level were therefore performed using the computational parameters described in the experimental section and the geometrical data reported in this work.

Selected net atom charges and bond overlap populations for all four species studied are shown in Figure 5. Some values for orbital occupation in the metal are reported in Table VII while overlap population values for the chelate ring are split into their σ and π contributions in Table VIII.

Orbital interaction diagrams for the four compounds are shown in Figures 6 and 7. The low symmetry of the molecules (C_i) prevented an assignation of symmetry for each one of the molecular orbitals. However the diagrams can be analyzed from the MO of the ligands and the five "d" valence orbitals of the metal, labeling them a′ or a″, depending on whether the orbital is symmetric or antisymmetric with respect to the mirror plane xz.

Finally contour diagrams of the HOMO and LUMO of complexes **1a**, **2**, and **3** are shown in Figure 8.

Discussion

Visible–UV absorption spectra of compounds **1–3** show several bands difficult to assign, as has been reported,[4,5] nevertheless, the band around 16 000 cm^{-1} could be assigned to the transition $^1A_{2g} \leftarrow {}^1A_{1g}$ and the band around 23 000 cm^{-1} to the transition $^1B_{1g} \leftarrow {}^1A_{1g}$, which has been assigned as a charge-transfer transition band.[25c]

Structure. The behavior of the salicylaldimine derivatives in both series of compounds (open chain[11] and cyclic ketals) regarding Ni–N bond lengths indicates that they have a character intermediate between those of 1,2- and 2,3-naphthaldimines. This is also observed in the planarity of the system since, in the case of **1–3** the salicylaldimine complex has a step height intermediate between those of the corresponding 1,2- and 2,3-naphthaldimines.

This intermediate character is what had been observed in the determination of stability constants of the anionic hydroxy aldehydate complexes.[12] Therefore, a relationship between these parameters (Ni–N bond lengths and planarity of the system) and the stability of the complex could be assumed.

Several explanations have been proposed in order to account for the distortion from planarity observed in most salicylaldimine and naphthaldimine square-planar metal complexes. One of such explanations has been the steric one in which stepping is believed to occur in order to allow more clearance between groups bonded to the imine nitrogen.[4]

However, in this case the N substituent remains constant in all three complexes, and the stepping in **1** and **3** cannot be assigned to steric effects since **2** is almost planar. On the other hand, packing effects could be partly responsible for distortions since

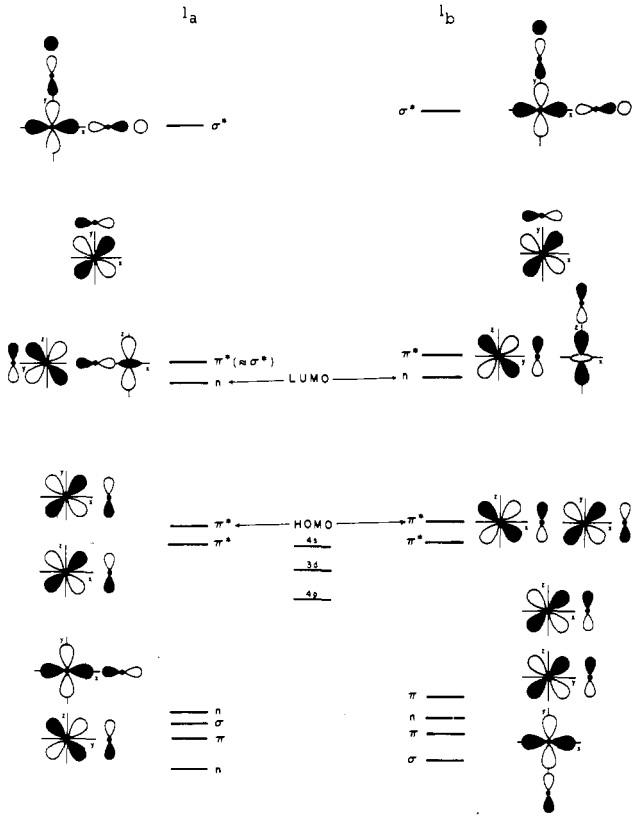

Figure 6. Interaction diagrams for **1a** and **1b**.

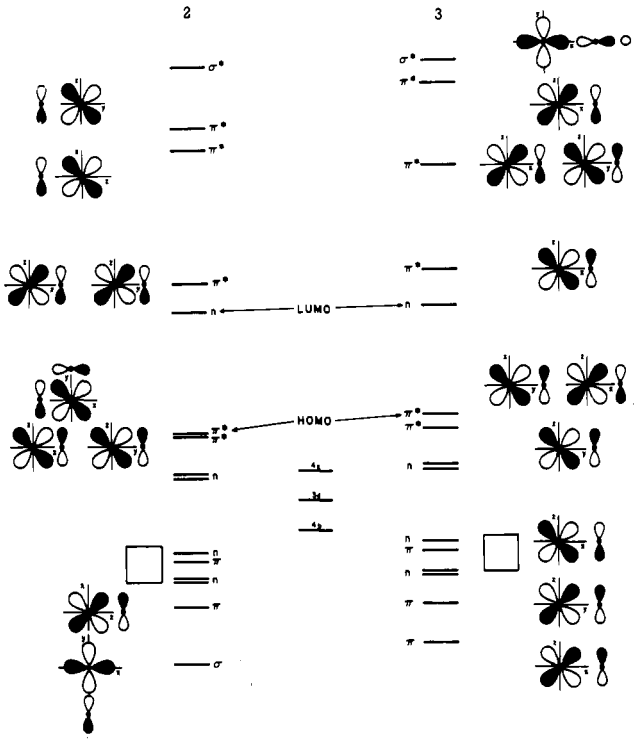

Figure 7. Interaction diagrams for **2** and **3**.

the different arrangement of the N substituent in **1a** and **1b** is accompanied by a variation in the height of the step although no close intramolecular contacts were observed in either case. In Figure 4 a side view of the four molecules can be observed.

Stepping in the Cu–naphthaldimine complexes has been related to solvent interactions.[10c] The absence of such interactions was assumed to reduce the electron density on oxygens, thus favoring a distortion in order to fulfill a necessity for an increased coordination sphere at copper. Interactions between metal and oxygen

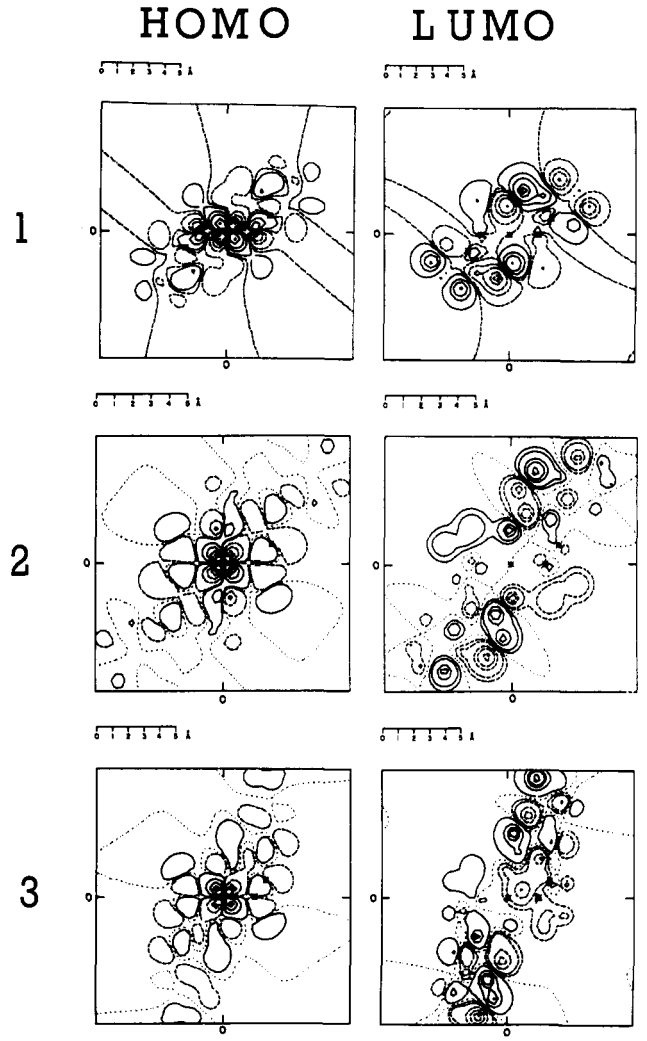

Figure 8. Contour diagrams for the HOMO and LUMO orbitals of compounds **1–3**.

atoms in neighboring molecules suggested this explanation,[10b,c] but as was noted above, no intramolecular interactions of this type were observed in either **1**, **2**, or **3**. Waters[6] also suggested that a larger angle at M–O(1)–C(2) could be attributed to a larger planarity of the molecule, which enhances double bonding of the oxygen to the metal; compound **2** does show a larger angle N(1)–O(1)–C(2) and is more planar than **1a**, **1b**, and **3**, but no shortening of the O(1)–Ni bond is observed.

EHMO Calculations. An alternation of charges in the chelate ring is observed in the four molecules, a behavior that had been previously reported.[31,32] The oxygen atom is the one with the largest negative charge followed by the nitrogen atom and one of the carbon atoms of the aromatic ring in that order. The most electrodeficient atoms in decreasing order are the metal atom, the carbon atom of the aromatic ring that is bonded to oxygen, and the imine carbon atom (Figure 5). These charges and the occupation of the metal orbitals vary from one compound to the other with the negative charge on nitrogen and the positive charge on the metal following the order **2** > **1a** > **1b** > **3**. The charge on the oxygen atom shows the reverse order, **3** > **1b** > **1a** > **2**. This distribution of charges suggests that the oxygen atom bonded to the metal could be the preferred site for an electrophilic attack, especially in the case of compound **3**.

An analysis of the electronic population of the metal orbitals shows that occupation of the $d_{x^2-y^2}$ orbitals of compound **2** (Table VII) is smaller than that calculated for the other compounds. On the other hand this molecule is also the one with the largest

(31) Cotton, F. A.; Harris, C. B.; Wise, J. J. *Inorg. Chem.* **1967**, *6*, 909.
(32) De Alti, G.; Galasso, V.; Bigotto, A. *Inorg. Chim. Acta* **1972**, *6*, 153.

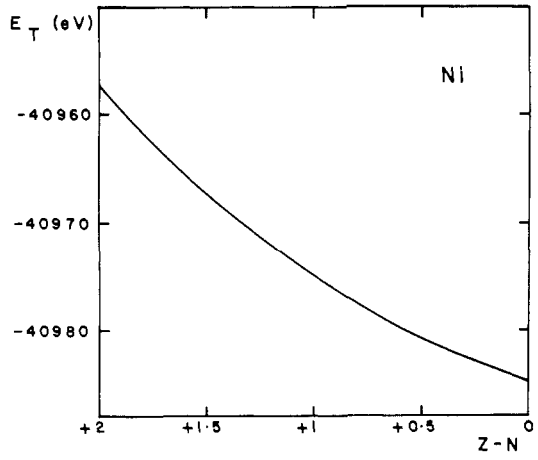

Figure 9. Plot of total energy vs. atomic charge of the nickel atom.

occupation of the d_{yz} orbital. This is probably due to the planarity of the molecule; in fact the orbital interaction diagram is very similar to the model for a square-planar compound.[33]

Overlap population values indicate larger electronic populations on the chelate ring bonds in compound **2**. The complete order observed is **2** > **1a**–**1b** > **3**. It can be assumed that in **2** there is a larger electronic delocalization from the aromatic rings toward the chelate ring favored by the great planarity of the compound. In this way the electronic population on the C–O bond of the chelate ring in compound **2** is larger than those in the other three molecules, which follow the order mentioned above.

The C–N bond presents a double-bond character in all the compounds, especially localized in **3**. This is further proved when the overlap populations in the chelate rings are divided into their σ and π contributions. So it can be observed in Table VIII that the largest π contribution to the C–N bond is found in compound **3**. In all three compounds both σ and π contributions to the C–N bond are larger than those to the C–O bond. On the other hand, σ contributions to the Ni–N bond are larger than those to the Ni–O bond, showing the better donor ability of the nitrogen atom. The π contributions to the Ni–N bond are small, which contrasts with the small negative values in the Ni–O bond that in compounds **1a** and **1b** are probably a result of antibonding interactions of the oxygen p_y and p_z orbitals with the metal d_{xy} and d_{xz} orbitals, respectively. This same type of interaction is observed in compounds **2** and **3** between p_x and p_y orbitals of the oxygen atoms and the metal d_{xy} and d_{yz} orbitals, respectively.

Interaction diagrams (Figures 6 and 7) show that the LUMO in the four cases is a nonbonding MO with ligand participation and the HOMO is a π^* orbital that interacts with ligand orbitals and also strongly with 2a′ as can be observed in the contour diagrams (Figure 8). The highest MO levels have σ^* character with 3a′ participation. In low-energy MOs of compounds **1a** and **1b** a different order can be observed, with the lowest MO in **1b** interacting with 3a′. On the other hand the LUMO's are essentially the same in both compounds, and the second lowest unoccupied π^* orbital interacts with 2a′ acquiring a small σ^* character.

A similar behavior is shown by compounds **2** and **3** with the exception of the lowest MO, which is a very penetrated orbital with σ character in **2** and π character in **3**. Higher MO's show the same characteristics in both complexes. In **2**, however, there is a large proximity between the π^* orbitals (almost degeneracy) when they interact with 1a′ and 2a′ (Figure 7) while in **3** there is a significant separation between them. This can be explained in terms of the interactions between the nitrogen and oxygen and metal orbitals, which are important in **2** but less important in **3** where oxygen orbitals interact very weakly as can be appreciated in the corresponding contour diagrams (Figure 8). In both compounds an interaction of the low-energy nonbonding orbital with 2a′ is observed while the very high σ^* interacts with 3a′, which also interacts with the σ orbital in complex **2**.

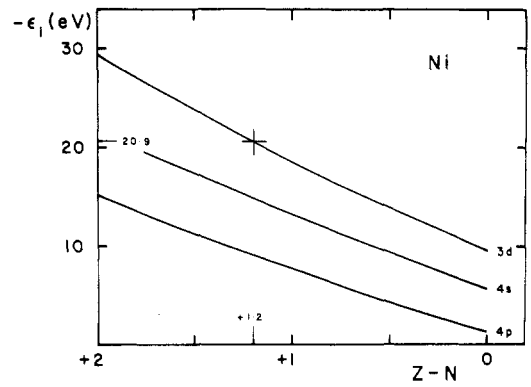

Figure 10. Plot of eigenvalues vs. atomic charge of the nickel atom.

If we finally look at the separation between energetic levels, the first transition is calculated around 10 000 cm^{-1} in the four cases, which agrees with the results reported by Maki[34] for a very low extinction band observed in the electronic spectra of complexes similar to the ones studied here.

Conclusions. While the chemistry of salicylaldimine complexes has been extensively studied, the corresponding hydroxynaphthaldimine derivatives have received very little attention. It could be thought nevertheless, that the behaviour of the naphthaldimine complexes would follow the same pattern as the salicylaldimine. This study shows that small differences in electronic factors between salicyladimines and 1,2- and 2,3-naphthaldimines play a significant role in the conformation of those complexes in the solid state.

Overlap populations and net atom charges, resulting from the EHMO calculations of the imine complexes here described, provide further insight into the electronic distribution of this type of compounds. They also seem to follow the same trend as that observed by Calvin and Wilson,[12] suggesting a close relationship between them. The net atom charge values on the oxygen atom coordinated to the nickel are consistent with the behavior observed in ligand substitution reactions studied by Elias et al.[7,8]

Additional studies in naphthaldimine complexes could give more light on the factors affecting the conformation of salicylaldimine complexes.

Acknowledgment. The authors thank Dr. B. F. G. Johnson and Dr. P. R. Raithby from the University of Cambridge for their help in the development of this project and Abelardo Cuellar for technical assistance.

Appendix

In this Appendix we describe the method employed to obtain the H_{3d3d} value for the nickel atom. The method is based on some recent results in density functional theory.[35] We have calculated the nickel atom within the Kohn–Sham formalism[36] using the local density approximation of Gunnarson and Lundquist[37] for the exchange and correlation contribution to the total energy.

The results obtained are shown in Figures 9 and 10 for the total energy and the eigenvalues as function of the atomic charge. From Figure 10 it can be seen that the value for the 3d energy level does not agree with the one used in the present calculation. The reason for this disagreement is that we are not describing properly the atomic state of the nickel atom in the molecule. In order to circumvent this deficiency, we incorporated the field produced by the neighbors closest to the nickel atom through the inclusion of a Watson sphere placed at a distance R = 1.9 Å and with charge −1.5. The radius of the Watson sphere was chosen as the average

(33) Huheey, J. E. *Inorganic Chemistry. Principles of Structure and Reactivity*, 3rd ed. (Harper International SI Edition); Harper: Mexico City, 1983; p 409.
(34) Maki, G. *J. Chem. Phys.* **1958**, *28*, 651.
(35) Gazquez, J. L.; Ortiz, E. *J. Chem. Phys.* **1984**, *81*, 2741.
(36) Kohn, W.; Sham, L. J. *Phys. Rev. A* **1965**, *140*, 1133.
(37) Gunnarsson, O.; Lundquist, B. I. *Phys. Rev. B: Solid State* **1976**, *B13*, 4274.

between the two closest distances to the nickel atom, and it can be seen that the charge (+1.5) is consistent with the Mulliken population analysis on the nickel atom found in the present EHMO calculations.

Certainly this method involves the appearance of two new parameters that could be avoided if we apply a charge iteration scheme using the results of a Kohn-Sham calculation instead of the usual iteration parameters. Work on this line is in progress and will be presented elsewhere.

Supplementary Material Available: Atom coordinates (Tables S1-S3), anisotropic temperature factors (Tables S4-S6), equations for least-squares planes (Table S7), atomic deviations from least-squares planes (Table S8), hydrogen coordinates (Tables S9-S11), and packing diagrams (Figures S1-S3) (15 pages); tables of observed and calculated structure factors (32 pages). Ordering information is given on any current masthead page.

Contribution from the Department of Chemistry, Laboratory for Molecular Structure and Bonding, Texas A&M University, College Station, Texas 77843, and Department of Chemistry, University of Texas at Austin, Austin, Texas 78712

Synthesis and X-ray Crystal Structures of $[Au(CH_2)_2PPh_2]_2(CF_3)_2$, $[Au(CH_2)_2PPh_2]_2(C_6F_5)_2$, and $[PPN][Au(C_6F_5)_4]$: Two Dinuclear Gold(II) Ylide Complexes Containing Alkyl and Aryl Ligands and a Tetrakis(pentafluorophenyl)aurate(III) Anion Complex

H. H. Murray,[†§] John P. Fackler, Jr.,*[†] Leigh C. Porter,[†∥] David A. Briggs,[†§] M. A. Guerra,[‡§] and R. J. Lagow[‡]

Received July 11, 1986

The reaction of $[Au(CH_2)_2PPh_2]_2Br_2$ with $Cd(CF_3)_2(glyme)$ in CH_2Cl_2 produces $[Au(CH_2)_2PPh_2]_2(CF_3)_2$, the first dialkyl Au(II) phosphorus ylide dimer to be structurally characterized. In both the solid state (X-ray) and solution (via ^1H NMR) the complex is symmetrically substituted along the Au(II)-Au(II) axis. The reaction of $Tl(C_6F_5)_2Cl$ with $[Au(CH_2)_2PPh_2]_2$ gives the diaryl Au(II) phosphorus ylide dimer $[Au(CH_2)_2PPh_2]_2(C_6F_5)_2$, which also has been structurally characterized by single-crystal X-ray diffraction. In solution (via ^1H NMR) as well as in the solid state (X-ray) this complex is also symmetrically substituted along the Au(II)-Au(II) axis. The preparation and X-ray crystal structure of the Au(III) anion $[Au(C_6F_5)_4]^-$ as the PPN salt is described. For $[Au(CH_2)_2PPh_2]_2(CF_3)_2$: monoclinic, $C2/c$ (No. 15), a = 13.194 (6) Å, b = 12.882 (7) Å, c = 17.609 (8) Å, β = 103.62 (4)°, Z = 4, R = 0.0231, R_w = 0.0233 for 1492 reflections with $F_o > 3\sigma(F_o^2)$ and 221 refined parameters. For $[Au(CH_2)_2PPh_2]_2(C_6F_5)_2$: triclinic, $P\bar{1}$ (No. 2), a = 11.822 (4) Å, b = 12.450 (4) Å, c = 20.232 (6) Å, α = 90.42 (3)°, β = 105.67 (3)°, γ = 103.18 (3)°, Z = 3, R = 0.0422, R_w = 0.0416 for 4532 reflections with $F_o > 3\sigma(F_o^2)$ and 322 refined parameters. For $[(Ph_3P)_2N][Au(C_6F_5)_4]$: orthorhombic, *Pbca* (No. 61), a = 19.130 (5) Å, b = 29.733 (6) Å, c = 19.296 (5) Å, Z = 8, R = 0.0552, R_w = 0.0580 for 3024 reflections with $F_o > 3\sigma(F_o^2)$ and 332 refined parameters.

Introduction

The gold(I) phosphorus ylide dimer $[Au(CH_2)_2PPh_2]_2$ (**1**) has several properties that make it a good model for physical[1] and theoretical[2] studies of bimetallic organometallic systems. It has proved to be a system that displays interesting features of structure[3] and reactivity.[4,5] Complex **1** contains a pair of two-coordinate Au(I) metal centers constrained in an eight-membered heterocyclic ring. The metal centers are electronically and sterically unsaturated, yet are held closely enough together to allow for a Au···Au interaction.[6] Complex **1** undergoes a facile two-center two-electron oxidative addition with halogens (for example Br_2) and pseudohalogens (for example benzoyl peroxide) acquiring two ligands and a Au(II)-Au(II) bond with each four-coordinate metal center in a fused five-membered heterocyclic ring, $[Au(CH_2)_2PPh_2]_2Br_2$ (**2**). These diamagnetic Au(II) centers remain electronically and sterically unsaturated and can undergo further oxidative addition, giving a dimer containing two Au(III) four-coordinate metal centers, $[Au(CH_2)_2PPh_2]_2Br_4$ (**3**).

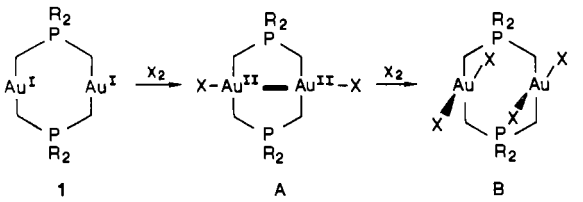

Complex **1** also shows facile oxidative addition with alkyl halides, RX, to give an asymmetrically substituted Au(II) dimeric species $[Au(CH_2)_2PPh_2]_2RX$ (**4**) that is in equilibrium[1] with **1**. These alkyl halide complexes give a Au-X bond length significantly longer than observed in the Au(II) symmetrically sub-

* To whom correspondence is to be addressed.
† Texas A&M University.
‡ University of Texas at Austin.
§ Syntheses.
∥ Crystallography. Present address: Argonne National Laboratory, Argonne, IL 60439.

(1) Fackler, J. P., Jr.; Murray, H. H.; Basil, J. D. *Organometallics* **1984**, *3*, 821.
(2) Basil, J. D.; Murray, H. H.; Fackler, J. P., Jr.; Tocher, J.; Mazany, A. M.; Delord, T. J.; Bancroft, B. T.; Knachel, H.; Dudis, D. S.; Marler, D. O. *J. Am. Chem. Soc.* **1985**, *107*, 6908.
(3) Murray, H. H.; Mazany, A. M.; Fackler, J. P., Jr. *Organometallics* **1985**, *4*, 154.
(4) Fackler, J. P., Jr.; Murray, H. H.; Mazany, A. M. *Organometallics* **1985**, *3*, 1310.
(5) Murray, H. H., III; Fackler, J. P., Jr.; Tocher, D. A. *J. Chem. Soc., Chem. Commun.* **1985**, 1278.
(6) Fackler, J. P., Jr.; Basil, J. D. In *Inorganic Chemistry: Toward the 21st Century*; Chisholm, M. H., Ed.; ACS Symposium Series 211; American Chemical Society: Washington, DC, 1983; p 201-209.

0020-1669/87/1326-0357$01.50/0